JOURNAL OF APPLIED ELECTROCHEMISTRY 4 (1974) 109–115

A mathematical model for the porous lead dioxide electrode. II. The pseudo-steady state approach for low rates of discharge

DANIEL SIMONSSON

Department of Chemical Technology, The Royal Institute of Technology, S-100 44 Stockholm 70, Sweden

Received 17 September 1973

A theoretical analysis of the discharge behaviour of the porous lead dioxide electrode at low current densities is made on the basis of a previously proposed model. The pseudo-steady state approach proves to be useful for low rates of discharge, while it fails for rapid discharges.

The current distribution at low rates of discharge becomes non-uniform during discharge because of concentration changes and decreasing porosity.

The maximum of the current distribution moves inwards into the electrode during discharge, as a result of the gradual insulation of the electrode surface by lead sulphate crystals. At the end of a slow discharge the electrode material has been uniformly utilized along the depth of the electrode, provided that the porosity is sufficiently high. If, however, the initial porosity is less than about 50% the inner parts of the electrode may not always be fully utilized because of the extensive plugging of the pores by lead sulphate crystals.

1. Introduction

A dynamic model for the porous lead dioxide electrode was proposed in a previous paper [1], in which numerical calculations for high rates of discharge were reported. The rapid discharge is the most interesting case as regards transient behaviour, since the discharge capacity decreases with increasing current density. At low current densities the diffusion of acid into the pores is not a limiting factor so the electrode material can be utilized to a larger extent. Experimental studies of the porous lead dioxide electrode [2] have, however, indicated that even at low rates of discharge the inner parts of the electrode are not always fully utilized.

The purpose of the present paper is to extend the previous analysis [1] to the discharge behaviour of the porous lead dioxide electrode at low rates of discharge.

In order to simplify this analysis the assumption of pseudo-steady state can be made. This is a common assumption in dynamic analyses of porous electrodes undergoing structural changes [3–6]. In this approach the concentration profile is assumed to adjust itself rapidly to the steady state corresponding to the actual state of discharge distribution. It is, however, difficult to predict when this approach is adequate, since the mass transfer transient process has been shown to be completed within a period ranging from 10 to 10^4 s, depending on the system [7]. In the present paper a comparison between the numerical results of the complete dynamic model and the corresponding pseudo-steady state model will therefore be made.

2. The pseudo-steady state model

2.1 *Formulation of the model*

The model used in the analysis has been described in a previous paper [1]. This model is complex to apply since a non-linear partial differential equation appears among the equations which describe the system. The mathematical problem can, however, be considerably simplified if the assumption of pseudo-steady state is made. In this approach the mass transfer transient process is assumed to be completed within a time which is short in comparison to the time needed to produce significant structural changes in the porous electrode. Mathematically this means that the time derivative for the concentration can be set equal to zero, and an ordinary differential equation is obtained instead of a partial differential equation. The computational problem is thus considerably simplified.

As a further simplification, in the case of low currents, the convective contribution to the mass transfer will be neglected, since calculations have shown that this term has a negligible effect on the results.

The following symbols will be used in the analysis:

a dimensionless parameter, $\frac{\kappa_0 RT}{ILF}$

b dimensionless parameter, $\frac{F(D_1-D_2)c_0}{IL}$

c concentration of sulphuric acid, kmol m^{-3}

c_o concentration of sulphuric acid in the bulk electrolyte, kmol m^{-3}

C dimensionless concentration, c/c_o

D_c diffusion coefficient, $m^2 s^{-1}$

D_o diffusion coefficient at the initial conditions, $m^2 s^{-1}$

D_i effective diffusion coefficient of species i, $m^2 s^{-1}$

E electrode potential, V

E' dimensionless potential, FE_c/RT

E_c reversible electrode potential at concentration c, V

f dimensionless parameter, $\frac{IL}{2FD_0c_0}$

F Faraday's constant, $96{\cdot}5 \cdot 10^6$ As (kg equiv^{-1})

g dimensionless parameter, $-\frac{S_0 j_0 L}{I} \exp(-2F\eta_{x=0}/RT)$

i dimensionless current density, i_2/I

i_2 current density in the pore electrolyte, Am^{-2}

I applied, geometric current density, Am^{-2}

j_o exchange current density, Am^{-2}

L the thickness of one symmetric half of the porous electrode, m

q_o initially available quantity of charge per unit volume (Asm^{-3})

R universal gas constant, joule (kmol deg)$^{-1}$

S specific active surface area, m^{-1}

S_o initially available active surface area, m^{-1}

t time, s

t_1 the transference number of the hydrogen ion

T temperature, K

V_p molar volume of $PbSO_4$, m^3 kmol^{-1}

V_r molar volume of PbO_2, m^3 kmol^{-1}

x distance co-ordinate from the symmetry plane of the porous electrode, m

X degree of discharge, $-\frac{1}{q_0}\int_0^t \frac{\partial i_2}{\partial x} dt$

X_{max} the maximum fraction of the electrode material that can be utilized

z dimensionless distance, x/L

ε porosity

ε_o initial porosity

η overvoltage, E-E_c, V

η' dimensionless overvoltage, $\frac{F(\eta-\eta_{x=0})}{RT}$

κ_c conductivity of the pore electrolyte, Ω^{-1} m^{-1}

κ_o conductivity of the pore electrolyte at initial conditions, Ω^{-1} m^{-1}

τ dimensionless time, $\frac{D_0 t}{L^2}$

Introducing the simplifications discussed above in Equation 28 in reference 1 leads to the following material balance for the steady state:

$$0 = (3-2t_1)f\frac{\partial i}{\partial z} + \frac{\partial}{\partial z}\left(\left(\frac{\varepsilon}{\varepsilon_o}\right)^p \frac{D_c}{D_o}\frac{\partial C}{\partial z}\right) \quad (1)$$

The boundary conditions at $z = 0$ are:

$i = 0$ and $\partial C/\partial z = 0$. Equation 1 can thus be integrated to:

$$\frac{\partial C}{\partial z} = -(3-2t_1)f\left(\frac{\varepsilon_o}{\varepsilon}\right)^p \frac{D_o}{D_c} i \qquad (2)$$

The effect of the decreasing porosity on the transport coefficients is taken into account by the factor $(\varepsilon/\varepsilon_o)^p$. The value of the exponent p will be discussed below.

The porosity, ε, varies according to the formula

$$\varepsilon = \varepsilon_o - \frac{V_p - V_r}{V_r}(1-\varepsilon_o)\, X \qquad (3)$$

where

$$X = -\frac{IL}{D_o q_o}\int_o^\tau \frac{\partial i}{\partial z}\, d\tau \qquad (4)$$

The current distribution at pseudo-steady state is described by Equations 27 and 29 in reference 1:

$$i = a\left(\frac{\varepsilon}{\varepsilon_o}\right)^p \frac{\kappa_c}{\kappa_o}\left(\frac{\partial E'}{\partial C}\frac{\partial C}{\partial z} + \frac{\partial \eta'}{\partial z}\right) - b\left(\frac{\varepsilon}{\varepsilon_o}\right)^p \frac{\partial C}{\partial z} \qquad (5)$$

$$\frac{\partial i}{\partial z} = g\left(1-\frac{X}{X_{max}}\right)\exp(-2\eta') \qquad (6)$$

Equation 5 gives an expression for the current density in the pores and Equation 6 expresses the rate of the electrode reaction per unit volume of the electrode.

The appropriate boundary conditions are:

at $z = 0$: $\eta' = i = \dfrac{\partial C}{\partial z} = 0$

at $z = 1$: $i = 1$, $C = 1$

As initial conditions at $t = 0$ are taken:

$$C(z, 0) = 1,\ X(z, 0) = 0$$

2.2 *Numerical procedure*

The equations above were solved in the following stepwise manner:

1. Starting from the given initial structural conditions, the current distribution at the steady state corresponding to these conditions is calculated by simultaneous integration of Equations 5 and 6. The concentration derivative in Equation 5 is replaced by the right-hand expression in Equation 2. The numerical integration is carried out by a fourth-order Runge-Kutta method. An iterative 'shot method' is used to solve the boundary value problem [1].
2. When the current distribution is known, the concentration profile at pseudo-steady state can be calculated by numerical integration of Equation 2.
3. The current distribution calculated above is assumed to prevail during the time increment, $\Delta\tau$, and the new values at time $\Delta\tau$ of the state of discharge and porosity are calculated by the use of Equations 3 and 4.
4. The current distribution and the concentration profile at the pseudo-steady state corresponding to the new structural conditions are calculated in the same way as in steps 1 and 2 above.

The described procedure is repeated for each successive time step until the electrode potential decreases rapidly and the execution is terminated due to numerical overflow.

2.3 *Comparisons with the complete dynamic model*

In order to investigate when the pseudo-steady state approximation is adequate, a comparison was made between the numerical results predicted by the complete dynamic model and the corresponding pseudo-steady state solutions. The equations of the complete dynamic model were solved by the implicit Crank-Nicolson method described previously [1]. The value of p was taken equal to one.

At high rates of discharge (e.g. -1000 Am^{-2}) it was not at all possible to obtain any pseudo-steady state solution. Previous calculations in which the structural changes were disregarded [1] have furthermore shown that the mass transfer transient process is not completed before the discharge is terminated. The basic assumption of the pseudo-steady state model is thus not fulfilled at high rates of discharge.

At low rates of discharge, on the other hand, the pseudo-steady state approach proves to be adequate. The results deviate appreciably from those of the complete model only during the first 5% of the total discharge time for 5 h and 20 h discharges (Fig. 1).

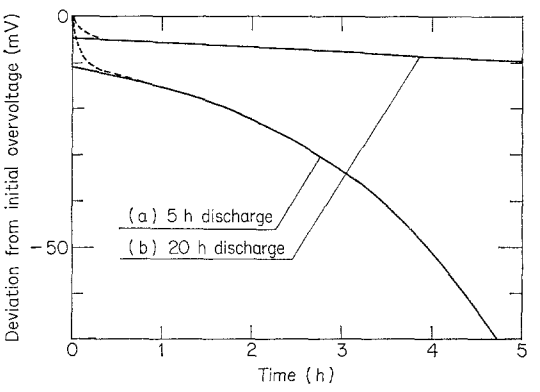

Fig. 1. Comparison between discharge curves predicted by the complete dynamic model (dashed lines) and the pseudo-steady state model (solid lines), ($\kappa_0 = 9\,\Omega^{-1}m^{-1}$, $\varepsilon_0 = 0{\cdot}50$; (a) $X_{max} = 0{\cdot}70$, (b) $X_{max} = 0{\cdot}80$. Other data, see reference [1]).

2.4 *The effect of the structural changes on the effective transport coefficients*

The molar volume of the reaction product – $PbSO_4$ – is about twice the volume of the reactant – PbO_2. The porosity thus decreases during discharge. Taking only the decreasing pore cross section into account would lead to a linear relation between the effective transport coefficients and the porosity. The value of p would then be equal to one. It is probable, however, that the tortuosity increases as a result of the precipitation of lead sulphate. A stronger dependence on the porosity than a linear one may thus be expected. The exponent p should best be regarded as an empirical constant which must be determined experimentally. In the case of the porous lead dioxide electrode, the effect of the structural changes on the transport parameters is complex. The changes in the effective conductivity due to the structural changes during discharge have been investigated experimentally [8].

The results indicate that the effective conductivity of the pore electrolyte is fairly constant during the first moments of discharge, while at higher degrees of discharge the conductivity decreases relatively more rapid than the porosity. A linear relation between the transport coefficients and the porosity is thus somewhat justified as a simple, average approximation when the extent of discharge is not too great, i.e. for rapid discharges. For low rates of discharge, on the other hand, a quadratic dependence on the porosity would be a better approximation [8]. A simple quadratic approximation, i.e. with $p = 2$, will therefore be used in the pseudo-steady state calculations for low rates of discharge.

3. Results and discussion

Calculations were carried out for $-25\ Am^{-2}$ (20 h discharge) and $-75\ Am^{-2}$ (5 h discharge). The numerical values of the parameters were the same as in [1]. The parameter X_{max} was used essentially as a fitting parameter. The influence of the porosity was investigated by varying this parameter without making any assumptions about how the other parameters are affected by a change in the initial porosity.

The shapes of the computed overvoltage-time curves were in agreement with experimental discharge curves.

The calculations for a 5 h discharge were interrupted when a local concentration of 0·5 M was reached in the interior of the electrode, since the basic approximations in the model become too rough below this value [1].

The changes in current distribution during discharge are shown in Fig. 2. The general

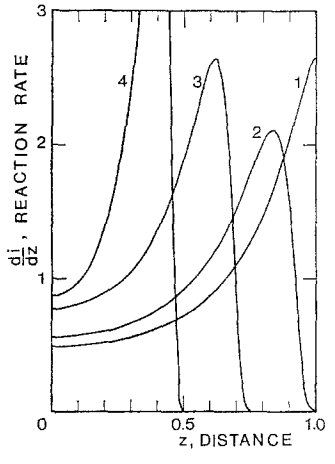

Fig. 2. Changes in current distribution during a 5 h discharge. ($X_{max} = 0{\cdot}70$, other data as in reference [1]) (1)77 min; (2) 155 min; (3) 232 min, (4) 284 min.

pattern is similar to that for high current densities [1]. During discharge a reaction zone advances from the front surface into the interior of the electrode.

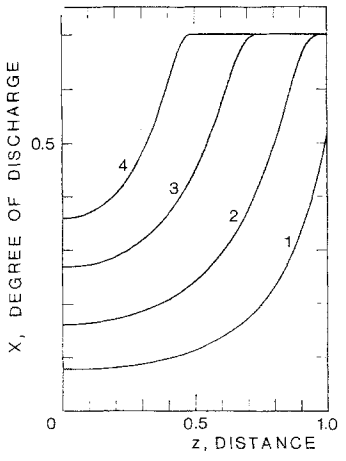

Fig. 3. Changes in the state of discharge distribution during a 5 h discharge. (X_{max} = 0·70, other data as in reference [1]). (1) 77 min; (2) 155 min; (3) 232 min; (4) 284 min.

Fig. 3 shows how the mass utilization is distributed along the depth of the electrode at different times during a 5 h discharge. The reaction zone can penetrate deeper into the electrode than at higher current densities. In this case, however, the material in the middle of the electrode cannot be utilized to its practical limit, before the discharge is terminated.

The acid concentration profile varies during a 5 h discharge according to Fig. 4. The increasing

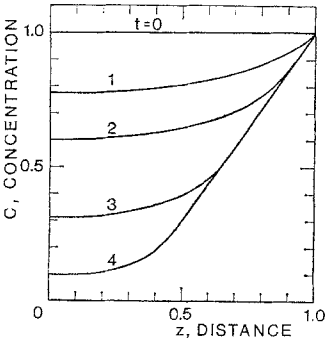

Fig. 4. Changes in the acid concentration profile during a 5 h discharge. (X_{max} = 0·70, other data as in reference [1]). (1) 77 min; (2) 155 min; (3) 232 min; (4) 284min.

mass transfer hindrance due to the decreasing porosity make the acid concentration in the middle of the electrode tend to very low values at the end of discharge.

At a 20 h discharge the electrode material can be utilized up to the practical limit (X_{max}) along the entire depth of the electrode, provided that the porosity is not too low (Fig. 5). The discharge

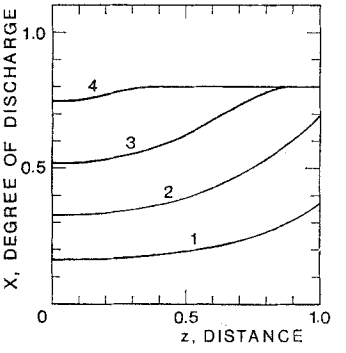

Fig. 5. Changes in the state of discharge distribution during a 20 h discharge. (X_{max} = 0·80, other data as in reference [1]). (1) 309 min; (2) 619 min; (3) 928 min; (4) 1134 min.

capacity is limited only by the passivation of the electrode surface by nonconducting lead sulphate crystals, and is thus proportional to the parameter X_{max}.

Under certain conditions an improved utilization (higher X_{max}) of the electrode material may, however, cause a reverse effect. At an initial porosity of 0·50 the discharge capacity is thus higher for X_{max} = 0·70 than for X_{max} = 0·80 (Fig. 6). This paradoxical phenomenon can be explained by Equation 3. According to this equation, the porosity decreases to very low

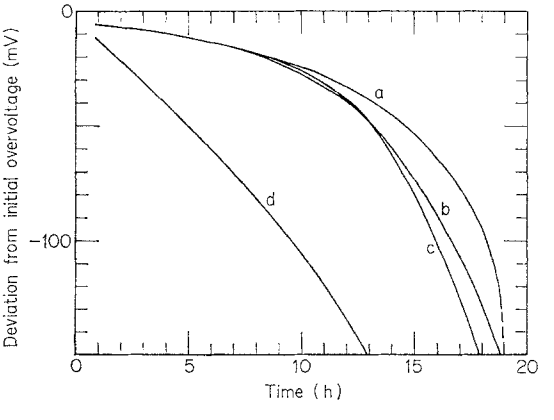

Fig. 6. Galvanostatic discharge curves for $I = -25 Am^{-2}$. (a) ε_0 = 0·60, X_{max} = 0·80; (b) ε_0 = 0·50, X_{max} = 0·70; (c) ε_0 = 0·50, X_{max} = 0·80; (d) ε_0 = 0·60, X_{max} = 0·80, $C(1,t) = 1 - 0{\cdot}04\,\tau$. Other data as in reference [1].

values when the initial porosity is low and, in addition, the parameter X can reach high values. Because of the extensive plugging of the pores, the interior of the electrode cannot be fully utilized before the discharge is terminated (Fig. 7). These results are sensitive to the value of the exponent p. With $p = 1{\cdot}5$ instead of 2 a uniform mass utilization is obtained.

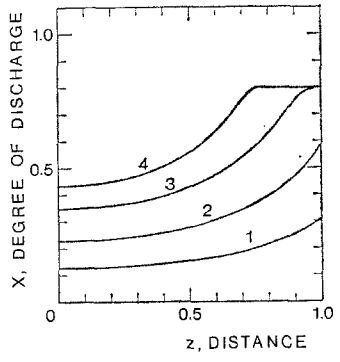

Fig. 7. Changes in the state of discharge distribution during discharge with -25 Am^{-2}. ($\varepsilon_0 = 0{\cdot}50$; $X_{max} = 0{\cdot}80$, other data as in reference [1]). (1) 309 min; (2) 567 min; (3) 876 min; (4) 1083 min.

The effective diffusion coefficient decreases during discharge due to the increasing structural hindrances. As a result, steep concentration gradients are established in the pores even at low rates of discharge. This aspect of the structural changes is important, since the concentration profile affects the potential profile in the electrolyte in a negative way – cf. Equation 5.

In the case discussed above (with $\varepsilon_0 = 0{\cdot}50$ and $X_{max} = 0{\cdot}80$) calculations have shown that the discharge can actually be continued if the concentration gradient is obliterated, e.g. with a forced electrolyte flow through the electrode. This effect has also been observed in practice [8].

In the cases discussed above the concentration of the bulk electrolyte is constant during discharge. In an actual battery, however, the concentration decreases during discharge. The magnitude of this decrease is determined mainly by the ratio between the initial amounts of sulphuric acid and electrode material.

To study the effect of a decreasing acid concentration in the bulk electrolyte a linear decrease with time was assigned to this variable. The concentration was assumed to decrease to about 1 M during the time which is equal to the obtained discharge time at constant acid concentration in the bulk electrolyte. Computations showed that under this condition, a 20 h discharge is instead terminated after about 15 h (Fig. 6), and a 5 h discharge is terminated after about 3 h, (when $\varepsilon_0 = 0{\cdot}60$ and $X_{max} = 0{\cdot}70$).

At the end of discharge the state of discharge distribution is fairly non-uniform along the depth of the electrode. The concentration in the bulk electrolyte is 2–3 M, while the concentration in the middle of the electrode tends to zero. This effect is still more pronounced for thicker electrodes.

4. Conclusions

At low rates of discharge the theoretical analysis of the dynamic behaviour of the porous lead dioxide electrode can be successfully simplified by the pseudo-steady state approach. The results indicate that the mass utilization is higher and more uniform along the depth of the electrode at lower rates of discharge. If the initial porosity is low (below 0·50) an improved local mass utilization may cause a decrease in discharge capacity due to the extensive plugging of the pores.

When the model is used to predict the performance of a positive plate in a battery, the decreasing concentration of sulphuric acid in the bulk electrolyte must be taken into account.

The original assumptions in the model may become fairly rough at the end of an extensive discharge with a low current density. At a 20 h discharge, the rate equation, Equation 6, is used at its lower limit of validity. The effective conductivity of the matrix phase may decrease much faster than that of the pore electrolyte. The conductivity of the electrode material, and its dependence on the local degree of discharge must then be taken into account.

The model can be improved when further knowledge is available about electrolytic data, the discharge mechanism, and the properties of the electrode material as functions of the local degree of discharge.

References

[1] D. Simonsson, *J. Appl. Electrochem.*, **3** (1973) 261.
[2] D. Simonsson, *J. Electrochem. Soc.*, **120** (1973) 151.

[3] R. Alkire, E. Grens and C. Tobias, *ibid.*, **116** (1969) 1328.
[4] J. Dunning, D. Bennion and J. Newman, *ibid.*, **118** (1971) 1251.
[5] R. Alkire and B. Place, *ibid.*, **119** (1972) 1687.
[6] J. Dunning, D. Bennion and J. Newman, *ibid.*, **120** (1973) 906.
[7] E. Grens and C. Tobias, *Ber. Bunsenges. Physik. Chem.*, **68** (1964) 236.
[8] M. Risberg, P. Sahleström and D. Simonsson, Report TRITA-KTE 1003, Royal Institute of Technology, Stockholm 1973.